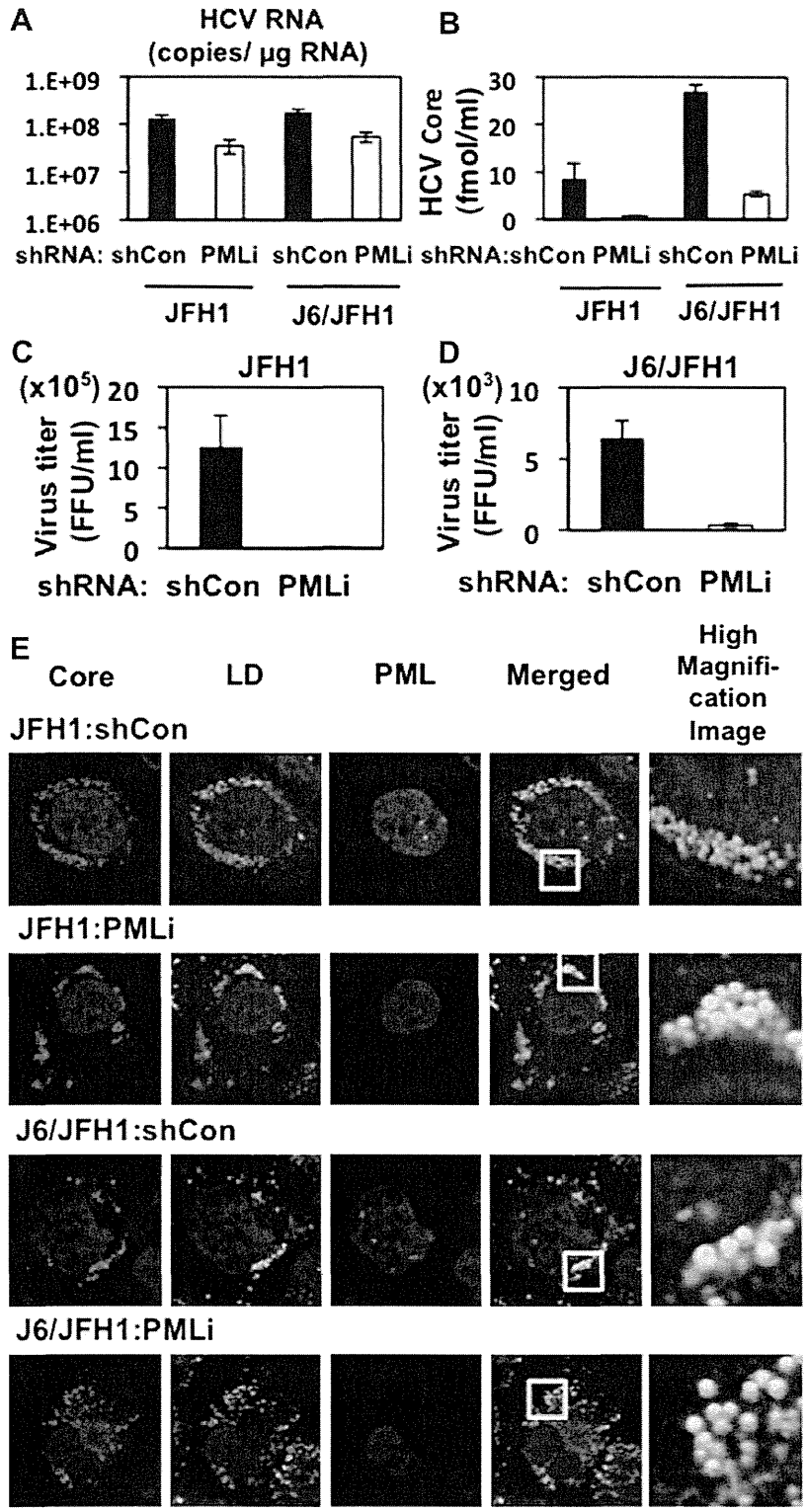

Fig. 3. PML is dispensable for the localization of HCV core to lipid droplet. (A) The levels of intracellular HCV RNA in PML knockdown or the control RSc cells 96 h after inoculation of HCV-JFH1 or HCV-J6/JFH1 were monitored by real-time LightCycler RT-PCR. Results from three independent experiments are shown (A–C). (B) The levels of HCV core in the culture supernatants from the PML knockdown RSc cells at 96 h post-infection were determined by ELISA. (C, D) The infectivity of HCV in the culture supernatants was determined by a focus-forming assay at 48 h post-infection. (E) HCV core localizes to lipid droplet (LD) in the PML knockdown (PMLi) or the control (shCon) cells after infection with either HCV-JFH1 or HCV-J6/JFH1. Cells were fixed 72 h post-infection and were then examined by confocal laser scanning microscopy.

3.2. PML is unrelated to HCV RNA replication

To examine whether or not PML is involved in HCV RNA replication, we used the subgenomic replicon RNA of HCV-JFH1, JRN/3-5B, encoding *Renilla* luciferase gene for monitoring the HCV RNA replication (Fig. 2A). *In vitro* transcribed JRN/3-5B RNA was transfected into the PML knockdown OR6c cells by electroporation and we examined the luciferase activity. Consequently, the

luciferase activity in the PML knockdown cells was similar to that of the control cells (Fig. 2B), indicating that shRNA targeted to PML could not affect the transient HCV RNA replication. As well, the level of HCV RNA in PML knockdown HuH-7-derived OR6c JRN/3-5B cells harboring the subgenomic replicon RNA of HCV-JFH1 and the cell growth was not affected (Fig. 2C and D), suggesting that PML is unrelated to the HCV RNA replication. To further confirm whether or not PML is involved in HCV production, we used *trans*-packaging system [21,22], that HCV subgenomic replicon was efficiently encapsidated into infectious virus-like particles by expression of HCV core to NS2 coding region. In fact, infectious HCV-like particles were produced and released into the culture medium from PML knockdown JRN/3-5B cells stably expressing core to NS2 coding region of HCV-JFH1 genome by mouse retroviral vector (Fig. 2E). We could monitor the HCV RNA replication by *Renilla* luciferase assay in target naïve RSc cells after the inoculation of infectious HCV-like particles. Consequently, the release of infectious HCV-like particles into the culture supernatants was significantly suppressed in PML knockdown cells at 72 h post-infection (Fig. 2F). Thus, we conclude that PML is associated with HCV production.

3.3. PML is required for the late step in the HCV-JFH1 life cycle

To avoid the possibility of specific finding when we only used HCV-JFH1, we examined another strain of HCV-J6JFH1 [20]. For this, we analyzed the level of HCV core and the infectivity in the culture supernatant as well as the level of HCV RNA in the PML knockdown RSc cells 96 h after inoculation of HCV-J6/JFH1. In this context, the level of HCV RNA in PML knockdown cells was only somewhat decreased (Fig. 3A), while the level of core and the infectivity in the culture supernatants was remarkably reduced (Fig. 3B–D), indicating that PML is required for infectious HCV-J6/JFH1 production as well as HCV-JFH1.

Since lipid droplets have been shown to be involved in an important cytoplasmic organelle for HCV production [3], we performed immunofluorescence and confocal microscopic analyses to determine whether or not HCV core misses localization into lipid droplets in the PML knockdown cells. We found that the core protein was targeted into lipid droplets even in PML knockdown RSc cells as well as in the control RSc cells after infection with either HCV-JFH1 or HCV-J6/JFH1 (Fig. 3E). This suggests that PML plays a role in the late step after the core is targeted into lipid droplet in the HCV life cycle. Importantly, HCV did not disrupt the formation of PML-NBs in response to HCV infection (Fig. 3E) unlike HIV-1 and other DNA viruses [6,7,23].

3.4. INI1 and DDX5, PML-related proteins, are involved in HCV production

Finally, we established the INI1 or DDX5, PML-related protein [23,24], knockdown RSc or OR6c JRN/3-5B cells by lentiviral vector expressing shRNA target to INI1 [17] or DDX5 to examine potential role of INI1 and DDX5 in HCV life cycle. Consequently, we found that the release of HCV core or the infectivity of HCV into the culture supernatants was significantly suppressed in the INI1 or DDX5 knockdown RSc cells 96 h after HCV-JFH1 infection, while the RNA replication in the knockdown cells was only somewhat decreased in spite of the very effective knockdown of INI1 or DDX5 mRNA without growth inhibition (Fig. 4A–F), suggesting that INI1 and DDX5 are involved in HCV life cycle. To confirm whether or not these proteins are involved in HCV RNA replication, we examined the luciferase assay in the INI1 or DDX5 knockdown OR6c JRN/3-5B cells. In this context, the shRNA target to INI1 or DDX5 did not affect the luciferase activity and the cell growth in these knockdown cells (Fig. 4G and H), suggesting that both INI1 and DDX5 are required for HCV production like PML.

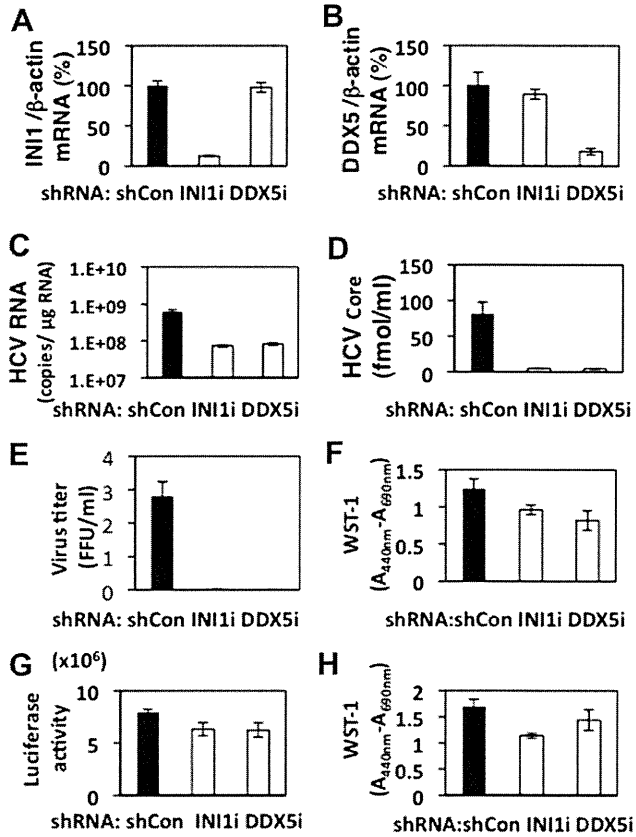

Fig. 4. INI1 and DDX5, PML-related proteins, are required for HCV production. (A, B) Inhibition of INI1 and DDX5 mRNA expressions by the shRNA-producing lentiviral vector. Real-time LightCycler RT-PCR for INI1 and DDX5 was performed as well as for β-actin mRNA in triplicate. Each mRNA level was calculated relative to the level in RSc cells transduced with a control lentiviral vector (Con) which was assigned as 100%. (C) The levels of intracellular genome-length HCV-JFH1 RNA in each knockdown cells at 96 h post-infection at an MOI of 0.05 were monitored by real-time LightCycler RT-PCR. (D) The levels of HCV core in the culture supernatants from the INI1 (INI1i) or DDX5 knockdown (DDX5i) RSc cells 96 h after inoculation of HCV-JFH1 were determined by ELISA. (E) The infectivity of HCV-JFH1 in the culture supernatants was determined by a focus-forming assay at 48 h post-infection. Virus titer is shown as ($x10^7$) FFU/ml. (F) WST-1 assay of each knockdown RSc cells at 96 h post-infection. (G) The HCV RNA replication level in INI1 and DDX5 knockdown OR6c JRN/3-5B cells was monitored by RL assay. (H) WST-1 assay of each knockdown OR6c JRN/3-5B cells. All results shown are means from three independent experiments.

4. Discussion

So far, the PML tumor suppressor protein, which forms PML-NBs, has been implicated in host antiviral defenses [6,7]. In fact, PML is induced by interferon after viral infection and suppresses some viral replication [6,7]. In contrast, PML-NBs are often disrupted or sequestered in the cytoplasm by infection with several DNA or RNA viruses to protect from the antiviral function of PML [6,7,23]. In case of HCV, Herzer et al. recently reported that the HCV core protein colocalizes with PML in PML-NBs and abrogates the PML function through interaction with PML isoform IV by over-expression studies [5]. However, we did not observe such colocalization of HCV core with PML and HCV did not affect the formation of PML-NBs in response to HCV-JFH1 infection (Fig. 3E). Interestingly, Watashi et al., previously demonstrated the HCV core modulates the retinoid signaling pathway through sequestration of

Sp110b, PML-related potent transcriptional corepressor of retinoic acid receptor, in the cytoplasm from nucleus [25].

In contrast, we have demonstrated that PML is required for infectious HCV production (Fig. 1). However, the molecular mechanism(s) how PML regulates HCV production yet remains unclear. At least, PML seems to be unrelated to the HCV RNA replication (Fig. 2). In this regard, several host factors including apolipoprotein E, components of ESCRT system, and PA28γ have been implicated in infectious HCV production [13,26,27]. Indeed, PA28γ, a proteasome activator, interacts with HCV core and affects nuclear retention and stability of the core protein. Importantly, PA28γ participates in the propagation of infectious HCV by regulation of degradation of the core protein [27]. Intriguingly, Zannini reported that PA28γ interacts with PML and Chk2 and affects PML-NBs number [28]. Accordingly, we demonstrated that ATM and Chk2, which phosphorylates PML and regulates the PML function, are involved in HCV life cycle [11]. In addition, other PML-related proteins such as INI1 and DDX5 seem to be involved in HCV production (Fig. 4). Indeed, INI1, also known as hSNF5, is incorporated into HIV-1 virion and is required for efficient HIV-1 production [29]. On the other hand, cytoplasmic PML may be involved in HCV production, since endoplasmic reticulum (ER) and lipid droplets are important cytoplasmic organelle for the HCV life cycle. In this regard, Giorgi et al. recently reported that cytoplasmic PML specifically enriches at ER [30], suggesting that cytoplasmic PML may be associated with HCV production. Altogether, the PML pathway seems to be involved in infectious HCV production.

Acknowledgments

We thank Drs. Didier Trono, Reuven Agami, Richard Iggo, Toshio Kitamura, Kenichi Abe and Apath LLC for the VSV-G-pseudotyped HIV-1-based vector system pCMVΔR8.91, pMDG2, pSUPER, pRDI292, Plat-E cells, pJRN/3-5B and pJFH1. We also thank Mr. Takashi Nakamura and Ms. Keiko Takeshita for their technical assistance. This work was supported by a Grant-in-Aid for Scientific Research (C) from the Japan Society for the Promotion of Science (JSPS), by a Grant-in-Aid for Research on Hepatitis from the Ministry of Health, Labor, and Welfare of Japan, and by the Viral Hepatitis Research Foundation of Japan. M. K. was supported by a Research Fellowship from JSPS for Young Scientists.

References

[1] N. Kato, Molecular virology of hepatitis C virus, Acta. Med. Okayama 55 (2001) 133–159.

[2] N. Kato, M. Hijikata, Y. Ootsuyama, et al., Molecular cloning of the human hepatitis C virus genome from Japanese patients with non-A, non-B hepatitis, Proc. Natl. Acad. Sci. USA 87 (1990) 9524–9528.

[3] Y. Miyanari, K. Atsuzawa, N. Usuda, et al., The lipid droplet is an important organelle for hepatitis C virus production, Nat. Cell Biol. 9 (2007) 1089–1097.

[4] D.R. McGivern, S.M. Lemon, Tumor suppressors, chromosomal instability, and hepatitis C virus-associated liver cancer, Annu. Rev. Pathol.: Mech. Dis. 4 (2009) 399–415.

[5] K. Herzer, S. Weyer, P.H. Krammer, et al., Hepatitis C virus core protein inhibits tumor suppressor protein promyelocytic leukemia function in human hepatoma cells, Cancer Res. 65 (2005) 10830–10837.

[6] R.D. Everett, M.K. Chelbi-Alix, PML and PML nuclear bodies: implications in antiviral defence, Biochimie 89 (2007) 819–830.

[7] E.L. Reineke, H.Y. Kao, Targeting promyelocytic leukemia protein: a means to regulating PML nuclear bodies, Intl. J. Biol. Sci. 5 (2009) 366–376.

[8] M. Kuroki, Y. Ariumi, M. Ikeda, et al., Arsenic trioxide inhibits hepatitis C virus RNA replication through modulation of the glutathione redox system and oxidative stress, J. Virol. 83 (2009) 2338–2348.

[9] T. Wakita, T. Pietschmann, T. Kato, et al., Production of infectious hepatitis C virus in tissue culture from a cloned viral genome, Nat. Med. 11 (2005) 791–796.

[10] Y. Ariumi, M. Kuroki, K. Abe, et al., DDX3 DEAD-box RNA helicase is required for hepatitis C virus RNA replication, J. Virol. 81 (2007) 13922–13926.

[11] Y. Ariumi, M. Kuroki, H. Dansako, et al., The DNA damage sensors ataxia-telangiectasia mutated kinase and checkpoint kinase 2 are required for hepatitis C virus RNA replication, J. Virol. 82 (2008) 9639–9646.

[12] Y. Ariumi, M. Kuroki, Y. Kushima, et al., Hepatitis C virus hijacks P-body and stress granule components around lipid droplets, J. Virol. 85 (2011) 6882–6892.

[13] Y. Ariumi, M. Kuroki, M. Maki, et al., The ESCRT system is required for hepatitis C virus production, PLoS One 6 (2011) e14517.

[14] M. Ikeda, K. Abe, H. Dansako, et al., Efficient replication of a full-length hepatitis C virus genome, strain O, in cell culture, and development of a luciferase reporter system, Biochem. Biophys. Res. Co. 329 (2005) 1350–1359.

[15] T.P. Brummelkamp, R. Bernard, R. Agami, A system for stable expression of short interfering RNAs in mammalian cells, Science 296 (2002) 550–553.

[16] A.J. Bridge, S. Pebernard, A. Ducraux, et al., Induction of an interferon response by RNAi vectors in mammalian cells, Nat. Genet. 34 (2003) 263–264.

[17] Y. Ariumi, F. Serhan, P. Turelli, et al., The integrase interactor 1 (INI1) proteins facilitate Tat-mediated human immunodeficiency virus type 1 transcription, Retrovirology 3 (2006) 47.

[18] L. Naldini, U. Blömer, P. Gallay, et al., In vivo gene delivery and stable transduction of nondividing cells by a lentiviral vector, Science 272 (1996) 263–267.

[19] R. Zufferey, D. Nagy, R.J. Mandel, et al., Multiply attenuated lentiviral vector achieves efficient gene delivery in vivo, Nat. Biotechnol. 15 (1997) 871–875.

[20] B.D. Lindenbach, M.J. Evans, A.J. Syder, et al., Complete replication of hepatitis C virus in cell culture, Science 309 (2005) 623–626.

[21] K. Ishii, K. Murakami, S.S. Hmwe, et al., Trans-encapsidation of hepatitis C virus subgenomic replicon RNA with viral structure proteins, Biochem. Biophys. Res. Co. 371 (2008) 446–450.

[22] E. Steinmann, C. Brohm, S. Kallis, et al., Efficient trans-encapsidation of hepatitis C virus RNAs into infectious virus-like particles, J. Virol. 82 (2008) 7034–7046.

[23] P. Turelli, V. Doucas, E. Craig, et al., Cytoplasmic recruitment of INI1 and PML on incoming HIV preintegration complexes: interference with early steps of viral replication, Mol. Cell 7 (2001) 1245–1254.

[24] G.J. Bates, S.M. Nicol, B.J. Wilson, et al., The DEAD box protein p68: a novel transcriptional coactivator of the p53 tumor suppressor, EMBO J. 24 (2005) 543–553.

[25] K. Watashi, M. Hijikata, A. Tagawa, et al., Modulation of retinoid signaling by a cytoplasmic viral protein via sequestration of Sp110b, a potent transcriptional corepressor of retinoic acid receptor, from the nucleus, Mol. Cell. Biol. 23 (2003) 7498–7509.

[26] K.S. Chang, J. Jiang, Z. Cai, et al., Human apolipoprotein E is required for infectivity and production of hepatitis C virus in cell culture, J. Virol. 81 (2007) 13783–13793.

[27] K. Moriishi, I. Shoji, Y. Mori, et al., Involvement of PA28γ in the propagation of hepatitis C virus, Hepatology 52 (2010) 411–420.

[28] L. Zannini, G. Buscemi, E. Fontanella, et al., REGγ/PA28γ proteasome activator interacts with PML and Chk2 and affects PML nuclear bodies number, Cell Cycle 8 (2009) 2399–2407.

[29] E. Yung, M. Sorin, A. Pal, et al., Inhibition of HIV-1 virion production by a transdominant mutant of integrase interactor 1, Nat. Med. 7 (2001) 920–926.

[30] C. Giorgi, K. Ito, H.K. Lin, et al., PML regulates apoptosis at endoplasmic reticulum by modulating calcium release, Science 330 (2010) 1247–1251.

培養細胞によるHBV感染増殖系の構築とその応用

土方　誠*

索引用語：B型肝炎ウイルス，培養肝細胞，感染，増殖，立体培養

1 はじめに

B型肝炎ウイルス(HBV)の感染者は世界中に約2億人存在すると推定されている．このウイルスの感染は急性肝炎や慢性の肝疾患の原因となっており，1982年に感染防御に効果的なワクチンが開発されている．またすでにHBVの遺伝子複製酵素の阻害剤が抗HBV薬剤として開発されている．しかしながら，それら薬剤に対する抵抗性変異株の出現も生じている．また，HBVは自然に宿主から完全に排除されることはない．HBV感染が治癒した場合でも，HBVが宿主免疫機能で抑制されているだけで，老化や免疫抑制剤の投与によってまたHBVの活動が再燃する可能性がある．一方，現在日本においては欧米型の遺伝子型AのHBVの感染が問題となっている．日本ではもともと遺伝子型CのHBVが主要なものであり，このHBVは成人に感染した場合，急性肝炎を引き起こすが，慢性化することは頻度が高くなかった．しかしながら，遺伝子型AのHBVは成人に感染した場合でも慢性化する割合が比較的高くなっている．したがって，このような問題を解決するためにも，HBVの感染増殖を効率良く抑制する新たな方法を開発することが必要とされている．またこのウイルスの感染によって引き起こされる肝炎や肝硬変，そして肝癌といった慢性肝疾患の発症の原因を解明し，これらを阻止するための方策を構築することも重要である．そのためにはHBVの慢性感染増殖や病原性を再現することが可能な培養細胞実験系が重要な役割を果たすことが考えられる．これまでわれわれの研究室ではヒトの肝臓に感染，増殖し，肝炎や肝硬変そして肝癌を発症するというHBVと多くの共通点をもつウイルスであるC型肝炎ウイルス(HCV)について，その感染増殖を再現する培養細胞系の開発を行ってきた．そこで本稿では，これら肝炎ウイルスが感染増殖する培養細胞系についてHBVを中心にしてこれまでの状況や知見を紹介しながら，今後の

Makoto HIJIKATA : Development and application of cell culture system for infection and proliferation of hepatitis B virus
*京都大学ウイルス研究所［〒606–8507 京都府京都市左京区聖護院川原町53］

表1

ウイルス / 細胞	HBV	HCV
初代培養ヒト肝細胞	培養初期に感染増殖感受性あり	培養初期に弱い感染増殖感受性あり
HepG2	感染増殖感受性なし* HBV DNAの導入で感染性粒子を産生可能	感染増殖感受性なし HCV受容体分子CD81を発現させると組換え体HCVの感染増殖が可能になる
HuH7	感染増殖感受性なし HBV DNAの導入で感染性粒子を産生可能	血清由来HCV感染増殖感受性なし 組換え体HCVの全生活環の高効率な再現可能 (亜株の使用による)
HepaRG	感染増殖感受性あり. DMSOやコルチゾルによる肝細胞様分化刺激が必要	感染増殖感受性あり. 肝細胞様分化で効率上昇
HuS-E/2	未検	通常の平面培養では低い感染増殖がみられる. 立体培養で肝細胞様分化が誘導され,全生活環の再現可能(効率は低い)
多能性幹細胞	未検	肝様細胞に分化された細胞は,組換え体HCVの全生活環の再現可能 血清由来HCV感染増殖感受性あり (効率は低い)

*感染増殖感受性ありの報告もある

HBV培養細胞実験系の展望について述べたい.

2 組換え体感染性HBVの産生

分類上HBVの属するヘパドナウイルスのウイルス学的なさまざまな知見は,HBVと近縁なアヒルHBVのアヒル初代培養肝細胞を用いた感染実験系によって得られているが,ここではヒトのHBVに関するヒト由来の培養細胞を用いた感染実験系に焦点をあてたい.HBVはHCVに比較してヒトに対する感染力が非常に強いウイルスであると考えられているが,培養細胞に関していえば,HBVが効率良く感染し増殖する細胞は決して多くない.これは同じヒト肝臓に感染するHCVと全く同じ状況である.現在までに各ウイルスの感染実験に用いられているヒト由来の代表的な細胞と各ウイルスとの関係を表1にまとめた.これまでにHBVの感染増殖実験に用いられた培養細胞には大別してヒト肝癌由来細胞と初代培養ヒト肝細胞が存在する.まず,いくつかのヒト肝癌由来細胞にHBV遺伝子DNAをトランスフェクションにより導入することで,組換え体HBV粒子を産生することが可能であることが1987年に相次いで報告された(図1)[1~3].特にヒト肝芽種由来細胞であるHepG2細胞にHBV遺伝子発現プラスミドを導入して得られた

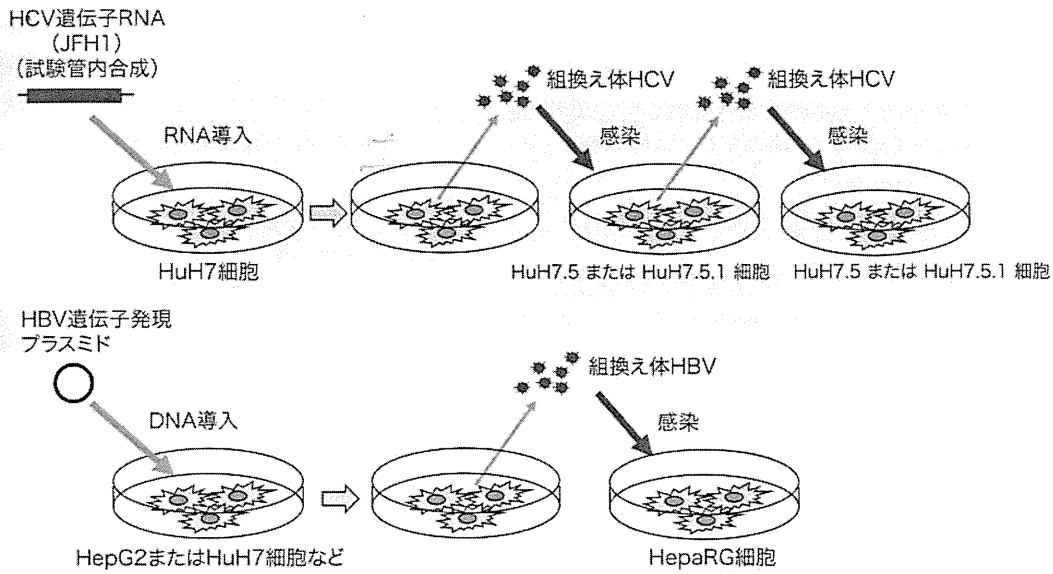

図1　HBVとHCVにおける組換え体ウイルスの産生と培養細胞を用いた感染実験の比較

HepG2クローン2.2.15細胞から産生されたHBV様粒子はHBVの感染モデル動物であるチンパンジーに感染し，急性の肝炎を引き起こした[4]．つまり，この細胞からは感染性を有する組換え体HBV粒子が産生されていることが示され，これ以降，HBVの感染実験の多くは同様の原理で作製された組換え体HBVを用いて進められている．例えば，以下のような研究も行われている．複製可能な最短の長さである1.24倍の長さをもつ種々の遺伝子型の組換え体HBV DNAゲノムをヒト肝癌由来細胞HuH7細胞に導入しそれぞれの遺伝子型のHBV粒子が得られた[5]．これらの組換え体HBV粒子の感染性は以下のような特殊な動物を用いて解析された．それは免疫不全マウスと自己肝臓がダメージを受けるような遺伝子を導入したトランスジェニックマウスの雑種マウスにヒト初代培養肝細胞を導入することで作製した，いわゆるヒト肝臓キメラマウスである．このキメラマウスの肝臓は大部分がヒトの肝細胞に置換しているため，ヒトの肝炎ウイルスの感染実験に用いることができる[6,7]．この方法により，上記の異なる遺伝子型HBV間の感染増殖性などの相違についても解析されている[8]．これらの組換え体HBVはその産生細胞自体にも感染しないため，感染実験にはこのような特殊な動物を用いる必要があった．つまり，この培養細胞を用いた実験系ではHBVのすべての生活環を再現することはできなかった．

3　HBVの感染が可能な培養細胞

HBVが効率良く感染することが期待されるのはもちろん，もともとHBVの感染標的であるヒトの肝臓組織から得た初代培養肝細胞である[9]．上記組換え体HBVは培養したヒト胎児肝細胞に感染，増殖し，この細胞からは感染性をもつウイルス様粒子が産生された[10]．つまり，この実験系を用いることにより，HBVの生活環がすべて再現されることになる．しかしながら，ヒト肝臓由来の初代培養肝細胞のHBV感染実験での使用にはい

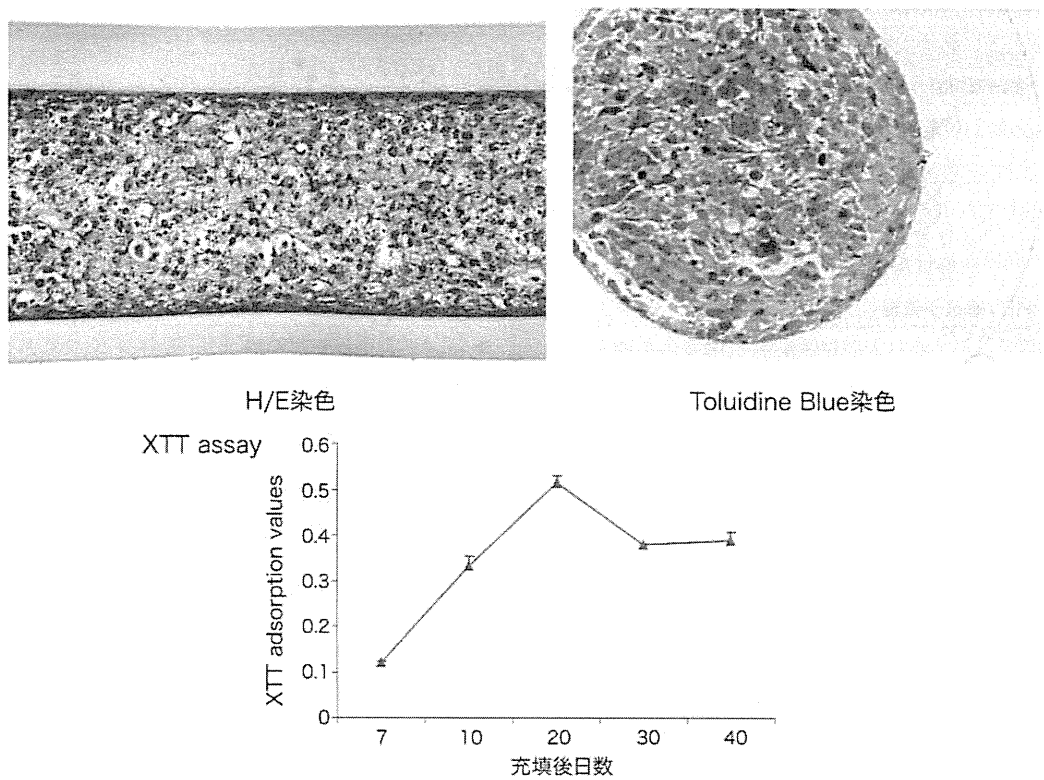

図2　中空糸に充填したHuS-E/2細胞の形態と細胞増殖

くつかの問題が存在する．まずヒトの組織から細胞を得る必要があるため，この細胞を入手することがすべての研究者にとって容易ではない．市販の細胞もあるが非常に高価であり，品質も安定していない．また，均質な状態のよい初代培養肝細胞を得ても，これを肝細胞の性質をすべて保ったまま長期間維持することが難しいことも大きな問題である．さらにヒト組織から分離した後，培養下では増殖はあまりしないため，実験の再現性を検証するために必要な細胞数の確保が容易ではない．また，異なるヒト由来の初代培養肝細胞を用いた場合，遺伝的な背景が異なり多様であるため，実験がその影響を受ける可能性が考えられる．最もこの点はHBV感染と宿主因子の関連を研究するためには利点となることも考えられる．以上のような種々の理由もあり，初代培養ヒト肝細胞は広く一般的にHBV感染実験に用いられてはいない．そのような中，2003年にHepaRG細胞と呼ばれるヒト肝癌由来の細胞株に上述したHepG2クローン2.2.15細胞由来の組換え体HBVが比較的効率良く感染増殖することが報告された[11]．この細胞はDMSOとコルチコイドを用いて，より肝細胞に類似した細胞に分化させてHBVの感染増殖実験に用いている．しかしながら，HepaRG細胞から感染性のHBVが産生されているという報告はなく，この細胞を用いてHBVの生活環をすべて再現することはできていない．したがって，現時点において培養細胞を用いたHBVの生活環の解析や抗HBV薬剤のスクリーニングや評価

は組換え体HBV粒子産生系とヒト初代培養肝細胞，あるいはHepaRG細胞を組み合わせて用いて行うようになっている．近年このHepaRG細胞は血清由来のHCVの感染にも感受性をもつことも報告されており[12]，やはりHBVとHCVの感染を許容する細胞に一定の共通性が存在することが示唆される．

4 今後の可能性

上述したようにヒト肝臓キメラマウスは組換え体も患者血清由来HBVも効率良く感染し，このマウスの血中には感染性のHBV粒子が放出される．HCVに関してもこのマウスを用いることにより感染増殖を再現することができる．しかしながら，このキメラマウスを用いた*in vivo*の感染実験からはウイルスの生活環の詳細な研究を行うことは困難である．またこのマウスは非常に高価であり，気軽に使用することも難しい．しかし，このマウスにおける結果を含めて，これまでに述べてきたことからいえることはこれらのウイルスがヒトの肝細胞に極めて良く適応しているため，本来のヒト肝臓内の肝細胞と極めて類似したなんらかの性質を有する細胞のみがこれらウイルスの生活環のすべてを支持することができると思われることである．

われわれはこれまでに独自の方法で初代培養ヒト肝細胞から不死化肝細胞を樹立し，それを立体培養することで血清由来のHCVの生活環を再現できることを示している[13]．その方法について，詳しくは2008年の本書特大号の特集，C型肝炎のすべて2009においてすでに述べているのでここでは省略するが，この細胞は1カ月以上の間，肝細胞様の性質を保ったまま中空糸の中で培養可能であった（その形態と細胞増殖の様子をXTTアッセイで検出したものを図2に示す）．そしてその間，効率はまだまだ高くないもののHCVの感染増殖そして粒子産生が再現された．この結果は，この培養細胞実験系がHBVにも応用可能であることを示唆しており，今後の検討課題となっている．この不死化肝細胞は通常の平面培養ではあまり効率の高い感染増殖は認められず，培地への粒子放出も観察されなかった．つまり立体培養することにより，そのようなことが可能になるなんらかの性質を獲得したことになる．このことはこれまであまり高いHBVの感染増殖を示さなかった細胞も立体培養などのように培養方法になんらかの工夫をすることによりHBVの感染増殖が可能になる可能性を示していると思われる．また最近，ヒト多能性幹細胞から肝細胞へ分化させた細胞を用いてHCVの感染増殖を効率良く再現したと報告されている[14,15]．この細胞は分化誘導されてから約3週間で老化に至るため，それ以上の長期にわたる感染増殖は今のところ難しいように思われるが，このヒト多能性幹細胞由来の肝細胞様細胞はやはりHBVの感染増殖培養細胞系への応用が期待できる細胞である．

5 HBV感染増殖培養細胞系の応用

ウイルスの感染増殖を再現する培養細胞実験系は目的によって最適なシステムが異なる．例えば，抗HBV薬のスクリーニングあるいは評価を行うのであれば，ハイスループットスクリーニングには不向きではあるが，まずは既存の感染性組換え体HBV粒子産生系とHepaRG細胞を用いた感染実験系でも可能であると思われる．また近年，マウス繊維芽細胞上にごく小さなヒト初代培養肝細胞集塊を形成させ，立体的に培養することでヒト肝細胞の性質を維持させて薬剤開発に用いる方法が報告された[16]．この培養方法は

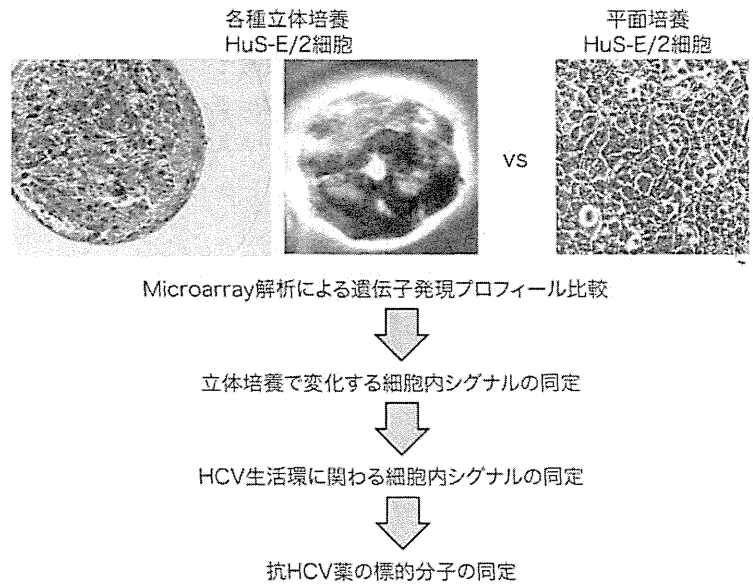

図3　異なる培養法による細胞の性質変化を利用した抗HCV薬の標的同定法

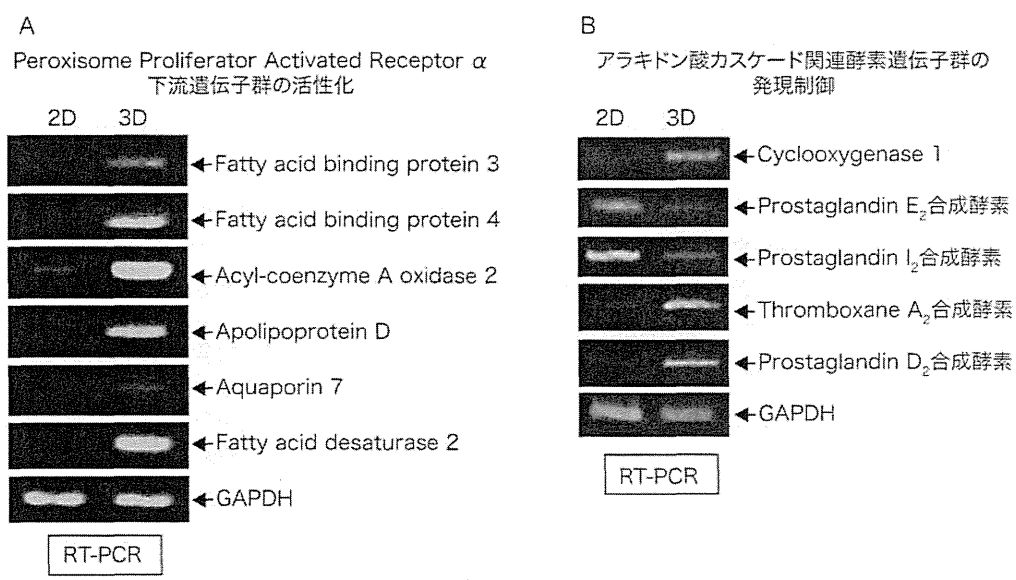

図4　立体培養HuS-E/2細胞で制御を受けた細胞内シグナル

HCVの感染実験にも応用することが可能であったため[17]，HBVの感染にも有望な培養細胞系であると考えられる．新しい抗HBV薬の薬効評価についてもヒト肝臓キメラマウスの前段階で安価に評価できる系として有用である．しかしながら，新薬の薬効の分子機構の解析には基礎的な解析が可能な，さらに感染増殖効率が高く，感染細胞数を多く得られる培養細胞系が必要となると考えられる．

培養方法の相違による感染増殖効率の違いをもとにHBV生活環の解析を行い，新たな抗HBV薬開発のための細胞側の標的因子を

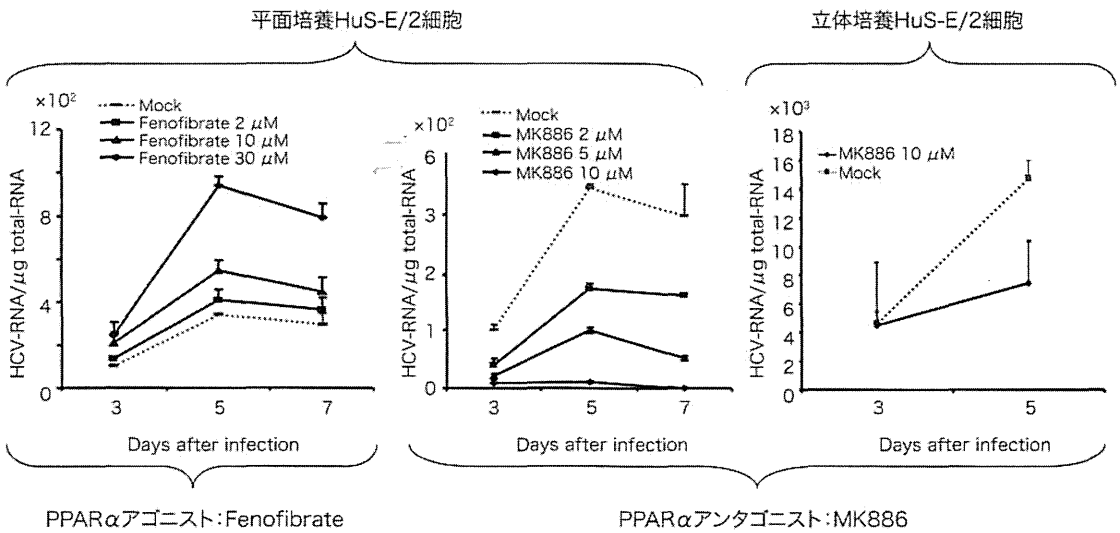

HCV:患者血液由来RC5, 遺伝子型1b

図5　PPARaアゴニストとアンタゴニストのHCV増殖に対する効果

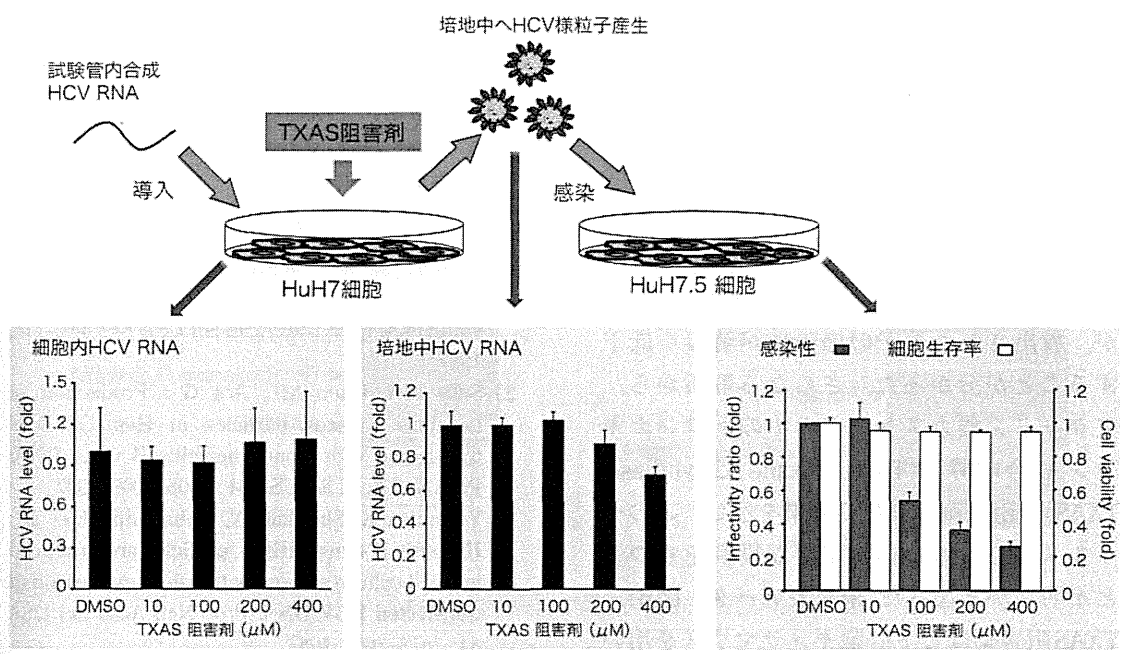

図6　TXAS阻害剤のHCV感染性粒子産生に対する効果

見いだすことも可能である．以下にHCVに関するものであるが参考までにわれわれの行ってきた研究を紹介する．上述したようにHuS-E/2細胞の立体培養系において平面培養時に比較して著しくHCVのゲノム複製効率が上昇することに着目して，平面培養から立体培養への変化でどのような細胞内の質的な変化が生じているのかを遺伝子発

現プロフィールをもとに解析した(図3)．その結果，肝細胞で重要な役割をもつペルオキシソーム増殖剤活性化受容体(Peroxisome Proliferator-activated receptor, PPAR) alphaのシグナルが立体培養によって著しく亢進していることを見いだした(図4A)[18]．PPAR alphaのアンタゴニストでこのシグナルを抑制すると感染した血清由来のHCVの増殖は抑制され，アゴニストでは逆に亢進されたことからこのシグナル系がHCVのゲノム複製に関与していることが分かり，このシグナルが抗HCV薬の標的となることが示唆された(図5)．この結果は後に別のグループによっても確認されている[19,20]．また最近，同様の方法で立体培養によってアラキドン酸カスケードの構成酵素遺伝子群の発現が制御され，初代培養肝細胞における発現に類似したものに変化していることを見いだした(未発表，図4B)．アラキドン酸カスケードの初発酵素であるシクロオキシゲナーゼ(cyclooxygenase , COX) 1の阻害剤で組換え体HCV粒子産生系を処理すると，HCVのゲノム複製や粒子の培地への放出は変化しないが，放出された粒子の感染性が著しく低下することが分かった．さらなる解析から，アラキドン酸カスケードの中のトロンボキサンA2合成酵素(Thromboxane A2 synthase, TXAS)の阻害剤が同様の効果を示し，このウイルスの感染性獲得に重要な役割をもつことが明らかとなった(未発表データ，図6)．TXAS阻害薬はヒト肝臓キメラマウスを用いた血清由来HCVの感染増殖を有意に抑制したことから新たな抗HCV薬の候補であることがわかった．同様の戦略はHBVの感染増殖を支持する細胞因子の解明にも十分に機能することが期待される．

6 おわりに

効率の高いHBV感染増殖培養細胞が開発されれば上述した過程以外にもその生活環のすべての過程を研究の対象にすることが可能になる．その中にはいまだ明らかになっていないHBVの肝細胞への感染に必要な受容体の同定も含まれる．またHBV感染増殖培養細胞はHBVの感染増殖に関連する研究に有用なだけではなく，HBV感染が引き起こす慢性の肝疾患，特に肝癌の解析にも有用である．そのためにはHBVの感染が長期にわたり観察できる培養細胞系が必要になると思われる．今後，HBV感染に苦しむ患者からHBVを排除し，また肝癌発症を防ぐ方法を確立するために，ヒト肝細胞の性質を長期に維持したまま培養することが可能な細胞培養系の早期開発が期待される．

文　献

1) Tsurimoto T, Fujiyama A, Matsubara K : Stable expression and replication of hepatitis B virus genome in an integrated state in a human hepatoma cell line transfected with the cloned viral DNA. Proc Natl Acad Sci USA 84 : 444–448, 1987
2) Sells MA, Chen ML, Acs G : Production of hepatitis B virus particles in Hep G2 cells transfected with cloned hepatitis B virus DNA. Proc Natl Acad Sci USA 84 : 1005–1009, 1987
3) Yaginuma K, Shirakata Y, Kobayashi M et al : Hepatitis B virus (HBV) particles are produced in a cell culture system by transient expression of transfected HBV DNA. Proc Natl Acad Sci USA 84 : 2678–2682, 1987
4) Acs G, Sells MA, Purcell RH et al : Hepatitis B virus produced by transfected Hep G2 cells causes hepatitis in chimpanzees. Proc Natl Acad Sci USA 84 : 4641–4644, 1987
5) Sugiyama M, Tanaka Y, Kato T et al : Influence of hepatitis B virus genotypes on the intra- and extracellular expression of viral DNA and antigens. Hepatology 44 : 915–924, 2006

6) Mercer DF, Schiller DE, Elliott JF et al : Hepatitis C virus replication in mice with chimeric human livers. Nat Med 7 : 927–933, 2001
7) Tsuge M, Hiraga N, Takaishi H et al : Infection of human hepatocyte chimeric mouse with genetically engineered hepatitis B virus. Hepatology 42 : 1046–1054, 2005
8) Sugiyama M, Tanaka Y, Kurbanov F et al : Direct cytopathic effects of particular hepatitis B virus genotypes in severe combined immunodeficiency transgenic with urokinase-type plasminogen activator mouse with human hepatocytes. Gastroenterology 136 : 652–662, 2009
9) Gripon P, Diot C, Thézé N et al : Hepatitis B virus infection of adult human hepatocytes cultured in the presence of dimethyl sulfoxide. J Virol 62 : 4136–4143, 1988
10) Ochiya T, Tsurimoto T, Ueda K et al : An in vitro system for infection with hepatitis B virus that uses primary human fetal hepatocytes. Proc Natl Acad Sci USA 86 : 1875–1879, 1989
11) Gripon P, Rumin S, Urban S et al : Infection of a human hepatoma cell line by hepatitis B virus. Proc Natl Acad Sci USA 99 : 15655–15660, 2002
12) Ndongo-Thiam N, Berthillon P, Errazuriz E et al : Long-term propagation of serum hepatitis C virus (HCV) with production of enveloped HCV particles in human HepaRG hepatocytes. Hepatology 54 : 406–417, 2011
13) Aly HH, Qi Y, Atsuzawa K et al : Strain-dependent viral dynamics and virus-cell interactions in a novel in vitro system supporting the life cycle of blood-borne hepatitis C virus. Hepatology 50 : 689–696, 2009
14) Schwartz RE, Trehan K, Andrus L et al : Modeling hepatitis C virus infection using human induced pluripotent stem cells. Proc Natl Acad Sci USA 109 : 2544–2548, 2012
15) Wu X, Robotham JM, Lee E et al : Productive hepatitis C virus infection of stem cell-derived hepatocytes reveals a critical transition to viral permissiveness during differentiation. PLoS Pathogens 8 : e-1002617, 2012
16) Khetani SR, Bhatia SN : Microscale culture of human liver cells for drug development. Nat Biotech 26 : 120–126, 2008
17) Jones CT, Catanese MT, Law LM : Real-time imaging of hepatitis C virus infection using a fluorescent cell-based reporter system. Nat Biotech 28 : 167–171, 2008
18) Aly HH, Shimotohno K, Hijikata M : 3D cultured immortalized human hepatocytes useful to develop drufs for blood-borne HCV. Biochem Biophy Res Commun 379 : 330–334, 2009
19) Gastaminza P, Whitten-Bauer C, Chisari FV : Unbiased probing of the entire hepatitis C virus life cycle identifies clinical compounds that target multiple aspects of the infection. Proc Natl Acad Sci USA 107 : 291–296, 2010
20) Chockalingam K, Simeon RL, Rice CM et al : A cell protection screen reveals potent inhibitors of multiple stages of the hepatitis C virus life cycle. Proc Natl Acad Sci USA 107 : 3764–3769, 2010

* * *

JVI
Journals.ASM.org

Japanese Encephalitis Virus Core Protein Inhibits Stress Granule Formation through an Interaction with Caprin-1 and Facilitates Viral Propagation

Hiroshi Katoh,[a] Toru Okamoto,[a] Takasuke Fukuhara,[a] Hiroto Kambara,[a] Eiji Morita,[b] Yoshio Mori,[d] Wataru Kamitani,[c] Yoshiharu Matsuura[a]

Department of Molecular Virology,[a] International Research Center for Infectious Diseases,[b] and Global COE Program,[c] Research Institute for Microbial Diseases, Osaka University, Osaka, Japan; Department of Virology III, National Institute of Infectious Diseases, Tokyo, Japan[d]

Stress granules (SGs) are cytoplasmic foci composed of stalled translation preinitiation complexes induced by environmental stress stimuli, including viral infection. Since viral propagation completely depends on the host translational machinery, many viruses have evolved to circumvent the induction of SGs or co-opt SG components. In this study, we found that expression of Japanese encephalitis virus (JEV) core protein inhibits SG formation. Caprin-1 was identified as a binding partner of the core protein by an affinity capture mass spectrometry analysis. Alanine scanning mutagenesis revealed that Lys^{97} and Arg^{98} in the α-helix of the JEV core protein play a crucial role in the interaction with Caprin-1. In cells infected with a mutant JEV in which Lys^{97} and Arg^{98} were replaced with alanines in the core protein, the inhibition of SG formation was abrogated, and viral propagation was impaired. Furthermore, the mutant JEV exhibited attenuated virulence in mice. These results suggest that the JEV core protein circumvents translational shutoff by inhibiting SG formation through an interaction with Caprin-1 and facilitates viral propagation *in vitro* and *in vivo*.

In eukaryotic cells, environmental stresses such as heat shock, oxidative stress, UV irradiation, and viral infection trigger a sudden translational arrest, leading to stress granule (SG) formation (1). SGs are cytoplasmic foci composed of stalled translation preinitiation complexes and are postulated to play a critical role in regulating mRNA metabolism during stress via so-called "mRNA triage" (2). The initiation of SG formation results from phosphorylation of eukaryotic translation initiation factor 2α (eIF2α) at Ser^{51} by various kinases, including protein kinase R (PKR), PKR-like endoplasmic reticulum kinase (PERK), general control nonrepressed 2 (GCN2), and heme-regulated translation inhibitor (HRI), which are commonly activated by double-stranded RNA (dsRNA), endoplasmic reticulum (ER) stress, nutrient starvation, and oxidative stress, respectively. Phosphorylation of eIF2α reduces the amount of eIF2-GTP-tRNA complex and inhibits translation initiation, leading to runoff of elongating ribosomes from mRNA transcripts and the accumulation of stalled translation preinitiation complexes. Thus, SGs are defined by the presence of components of translation initiation machinery, including 40S ribosome subunits, poly(A)-binding protein (PABP), eIF2, eIF3, eIF4A, eIF4E, eIF4G, and eIF5. Then, primary aggregation occurs through several RNA-binding proteins (RBPs), including T-cell intracellular antigen-1 (TIA-1), TIA-1-related protein 1 (TIAR), and Ras-Gap-SH3 domain-binding protein (G3BP). These RBPs are independently self-oligomerized with the stalled initiation factors and with other RBPs, such as USP10, hnRNP Q, cytoplasmic activation/proliferation-associated protein-1 (Caprin-1), and Staufen and with nucleated mRNA-protein complex (mRNP) aggregations (3, 4). SG assembly begins with the simultaneous formation of numerous small mRNP granules which then progressively fuse into larger and fewer structures, a process known as secondary aggregation (5). The aggregation of TIA-1 or TIAR is regulated by molecular chaperones, such as heat shock protein 70 (Hsp70) (3), whereas that of G3BP is controlled by its phosphorylation at Ser^{149} (4). SG formation and disassembly in response to cellular stresses are strictly regulated by multiple factors.

Viral infection can certainly be viewed as a stressor for cells, and SGs have been reported in some virus-infected cells. Since the propagation of viruses is completely reliant on the host translational machinery, stress-induced translational arrest plays an important role in host antiviral defense. To antagonize this host defense, most viruses have evolved to circumvent SG formation during infection. For example, poliovirus (PV) proteinase 3C cleaves G3BP, leading to effective SG dispersion and virus propagation (6). Influenza A virus nonstructural protein 1 (NS1) has been shown to inactivate PKR and prevent SG formation (7). In the case of human immunodeficiency virus 1 (HIV-1) infection, Staufen1 is recruited in ribonucleoproteins for encapsidation through interaction with the Gag protein to prevent SG formation (8). In contrast, some viruses employ alternative mechanisms of translation initiation and promote SG formation to limit cap-dependent translation of host mRNA (9, 10). In addition, vaccinia virus induces cytoplasmic "factories" in which viral translation, replication, and assembly take place. These factories include G3BP and Caprin-1 to promote transcription of viral mRNA (11).

Japanese encephalitis virus (JEV) belongs to the genus *Flavivirus* within the family *Flaviviridae*, which includes other mosquito-borne human pathogens, such as dengue virus (DENV), West Nile virus (WNV), and yellow fever virus, that frequently cause significant morbidity and mortality in mammals and birds (12). JEV has

Received 15 August 2012 Accepted 15 October 2012
Published ahead of print 24 October 2012
Address correspondence to Yoshiharu Matsuura, matsuura@biken.osaka-u.ac.jp.

doi:10.1128/JVI.02186-12

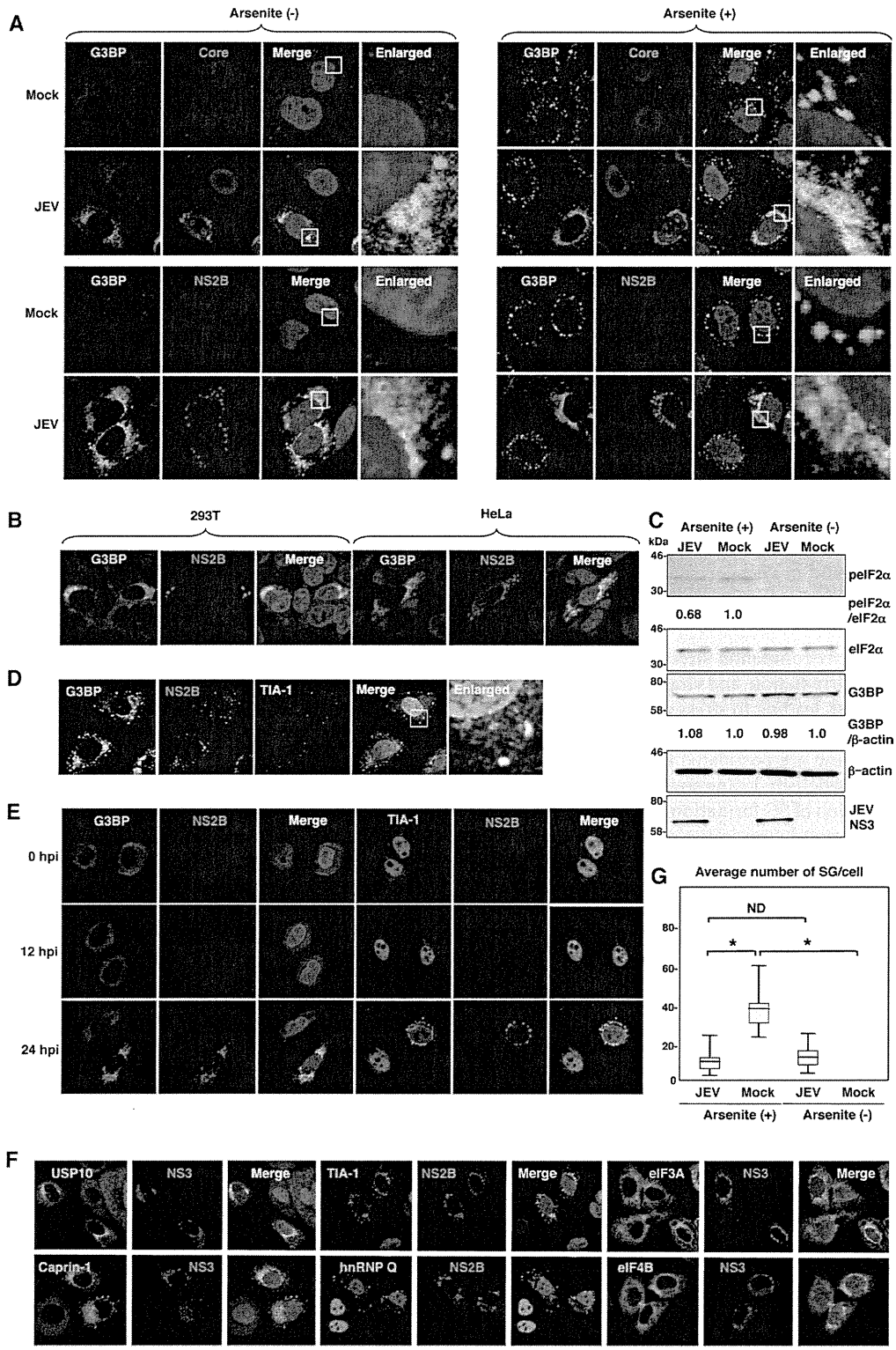

FIG 1 Dynamics of SG-associated factors during JEV infection. (A) Huh7 cells infected with JEV at an MOI of 0.5 were treated with or without 1.0 mM sodium arsenite for 30 min at 37°C, and the levels of expression of G3BP and JEV core protein/NS2B were determined at 24 h postinfection by immunofluorescence analysis with mouse anti-G3BP MAb and rabbit anti-core protein or anti-NS2B PAb, followed by AF488-conjugated anti-mouse IgG (Invitrogen) and AF594-conjugated anti-rabbit IgG, respectively. Cell nuclei were stained with DAPI (blue). (B) Cellular localizations of G3BP and JEV NS2B in 293T and HeLa cells infected with JEV were determined at 24 h postinfection by immunofluorescence analysis with mouse anti-G3BP MAb and rabbit anti-NS2B PAb, followed by AF488-conjugated anti-mouse IgG and AF594-conjugated anti-rabbit IgG, respectively. Cell nuclei were stained with DAPI (blue). (C) Phosphorylation of eIF2α in cells prepared as described in panel A was determined by immunoblotting using the indicated antibodies. The band intensities were quantified by ImageJ

a single-stranded positive-sense RNA genome of approximately 11 kb. The genomic RNA carries a single large open reading frame, and a polyprotein translated from the genome is cleaved co- and posttranslationally by host and viral proteases to yield three structural proteins, the core, precursor membrane (PrM), and envelop (E) proteins, and seven nonstructural (NS) proteins, NS1, NS2A, NS2B, NS3, NS4A, NS4B, and NS5 (13). PrM is further cleaved by the multibasic protease, furin, and matured to membrane (M) protein. The core, M, and E proteins are components of extracellular mature virus particles. NS proteins are not incorporated into particles and are thought to be involved in viral replication, which occurs in close association with ER-derived membranes (14). Previous reports have shown that WNV and DENV inhibit SG formation by sequestering TIA-1 and TIAR through specific interaction with viral RNA (15, 16). In addition, the membrane structure induced by WNV infection was suggested to prevent PKR activation and avoid induction of SG formation (17). In this study, we show that JEV core protein plays an important role in inhibition of SG formation. JEV core protein recruited several SG-associated proteins, including G3BP and USP10, through an interaction with Caprin-1 and suppressed SG formation. Furthermore, a mutant JEV carrying a core protein incapable of binding to Caprin-1 exhibited lower propagation *in vitro* and lower pathogenicity in mice than the wild-type (WT) JEV, suggesting that inhibition of SG formation by the core protein is crucial to antagonize host defense. These results reveal a novel strategy of JEV to inhibit SG formation through an interaction with Caprin-1 and facilitate viral propagation.

MATERIALS AND METHODS

Plasmids. Plasmids encoding FLAG-tagged JEV core protein (pCAGPM-FLAG-Core) and hemagglutinin (HA)-tagged JEV proteins (pCAGPM-HA-JEV proteins) were generated as previously described (18, 19). The cDNA of the core protein of JEV AT31 (amino acid residues 2 to 105) was amplified from the pCAGPM-FLAG-Core plasmid by PCR and cloned into pET21b (Novagen-Merck, Darmstadt, Germany) for expression in bacteria as a His-tagged protein and in pCAG-MCS2-FOS for expression in mammalian cells as a FLAG-One-STrEP (FOS)-tagged protein. The resulting plasmids were designated pET21b-Core-His and pCAG-Core-FOS, respectively. The cDNA of the core protein of DENV2 (amino acid residues 2 to 100) was amplified from the pCAG/FLAG-DEN2C-HA plasmid (19) by PCR and cloned into pCAGPM-N-FLAG. The cDNA of human Caprin-1 was amplified from 293T cells by reverse transcription-PCR (RT-PCR) and cloned into pCAGPM-N-HA (20) and pGEX 6P-1 (GE Healthcare, Buckinghamshire, United Kingdom) for expression in bacteria as a glutathione *S*-transferase (GST) fusion protein and designated pCAGPM-HA-Caprin-1 and pGEX-GST-Caprin-1, respectively. The cDNAs of human G3BP1 and USP10 were also amplified from 293T cells by RT-PCR and cloned into pCAGPM-N-HA. The nucleotide residues of the adenine at 384, adenine at 385, cytosine at 387, and guanine at 388 of the JEV genome in pMWATG1 were replaced with guanine, cytosine, guanine, and cytosine, respectively, by PCR-based mutagenesis to change Lys^{97} and Arg^{98} of the core protein to Ala, yielding pMWAT/KR9798A. The cDNA of the mutant core protein was also cloned into pCAGPM-N-FLAG and pET21b. To generate stable cell lines expressing *Aequorea coerulescens* green fluorescent protein (AcGFP)-fused Caprin-1, the cDNA of human Caprin-1 was amplified by RT-PCR and cloned into pAcGFP N1 (Clontech, Mountain View, CA), and the Caprin-1-AcGFP gene was subcloned into the lentiviral vector pCSII-EF-RfA (21) and designated pCSII-EF-Caprin-1-AcGFP. All plasmids were confirmed by sequencing with an ABI Prism 3130 genetic analyzer (Applied Biosystems, Tokyo, Japan).

Cells and stress treatment. Mammalian cell lines, Vero (African green monkey kidney), 293T (human kidney), Huh7 (human hepatocellular carcinoma), and HeLa (human cervical carcinoma), were maintained in Dulbecco's modified Eagle's minimal essential medium (DMEM) (Sigma, St. Louis, MO) supplemented with 100 U/ml penicillin, 100 mg/ml streptomycin, nonessential amino acids (Sigma), and 10% fetal bovine serum (FBS). The mosquito cell line C6/36 (*Aedes albopictus*) was grown in Leibovitz's L-15 medium with 10% FBS. Huh7 cells were transduced with a lentiviral vector expressing Caprin-1-AcGFP and AcGFP and designated Huh7/Caprin-1-AcGFP and Huh7/AcGFP, respectively. For induction of SGs, cells were treated with sodium arsenite at a final concentration of 1.0 mM in the culture medium for 30 min prior to fixation or lysis of the cells. SG formation was defined morphologically by immunostaining using anti-SG-related factor antibodies described below. Cell viability was determined by using CellTiter-Glo (Promega, Madison, WI) according to the manufacturer's instruction.

Viruses. The wild-type and 9798A mutant of the JEV AT31 strain were generated by the transfection of pMWATG1 and pMWAT/KR9798A, respectively, as described previously (22). Viral infectivity was determined by an immunostaining focus assay as described previously (20), and the results are expressed in focus-forming units (FFU). JEV and DENV serotype 2 New Guinea C strain were amplified in C6/36 cells.

Antibodies. Anti-JEV core rabbit polyclonal antibody (PAb) and anti-JEV NS3 mouse monoclonal antibody (MAb) were prepared as described previously (20, 23). Anti-JEV NS2B rabbit PAb was generated with synthetic peptides of JEV NS2B at Scrum, Inc. (Tokyo, Japan). Anti-DENV core protein rabbit PAb was prepared by using a GST-fused recombinant protein containing amino acid residues 2 to 100 of the DENV core protein. Anti-FLAG mouse MAb (M2) and rabbit PAb and anti-β-actin mouse MAb were purchased from Sigma. Anti-hnRNP Q mouse MAb (ab10687), anti-USP10 rabbit PAb (ab70895), and anti-eIF4B rabbit PAb (ab78916) were purchased from Abcam (Cambridge, United Kingdom). Anti-eIF2α, anti-phospho-eIF2α, and anti-eIF3A rabbit PAbs were purchased from Cell Signaling Technology (Danvers, MA). Anti-HA mouse MAb (HA11), anti-HA rat MAb (3F10), anti-His mouse MAb, anti-GFP mouse MAb (JL-8), anti-JEV envelope protein mouse MAb (6B4A-10), anti-G3BP mouse MAb, anti-TIA-1 goat PAb, anti-Caprin-1 rabbit PAb, and anti-dsRNA mouse MAb were purchased from Covance (Richmond, CA), Roche (Mannheim, Germany), R&D Systems (Minneapolis, MN), Clontech, Chemicon (Temecula, CA), BD Biosciences (Franklin Lakes, NJ), Santa Cruz (Santa Cruz, CA), Proteintech (Chicago, IL), and Bio-

software (NIH, Bethesda, MD), and the relative levels for the indicated proteins are shown based on the level of the mock-infected cells. (D) Cellular localizations of G3BP, NS2B, and TIA-1 in Huh7 cells infected with JEV were determined at 24 h postinfection by immunofluorescence analysis with mouse anti-G3BP MAb, rabbit anti-NS2B PAb, and goat anti-TIA-1 PAb, followed by AF488-conjugated anti-mouse IgG, AF594-conjugated anti-rabbit IgG, and AF633-conjugated anti-goat IgG, respectively. Cell nuclei were stained with DAPI (gray). (E) Dynamics of G3BP and TIA-1 during JEV infection. Huh7 cells infected with JEV were immunostained at 0, 12, and 24 h postinfection (hpi) with mouse anti-G3BP MAb or goat anti-TIA-1 PAb and rabbit anti-NS2B PAb, followed by AF488-conjugated anti-mouse IgG or AF488-conjugated anti-goat IgG and AF594-conjugated anti-rabbit IgG, respectively. Cell nuclei were stained with DAPI (blue). (F) Cellular localization of SG-associated proteins (USP10, Caprin-1, TIA-1, hnRNP Q, eIF3A, and eIF4B) (green, AF488-conjugated secondary antibody) and JEV NS2B/NS3 (red, AF-594-conjugate secondary antibody) in Huh7 cells infected with JEV was determined by immunoblotting at 24 h postinfection. Cell nuclei were stained with DAPI (blue). (G) Numbers of G3BP-positive foci in 30 cells prepared as described in panel A were counted for each experimental condition. Lines, boxes, and error bars indicate the means, 25th to 75th percentiles, and 95th percentiles, respectively. The significance of differences between the means was determined by a Student's *t* test.*, $P < 0.01$; ND, no significant difference.

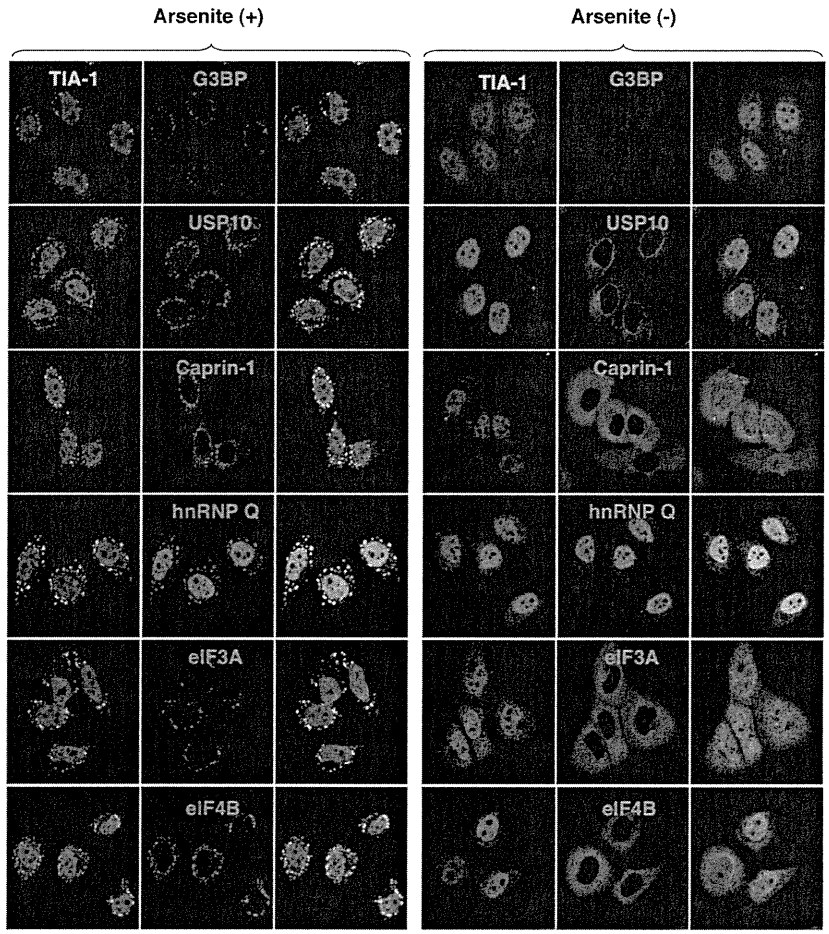

FIG 2 Each SG-associated factor forms SGs under oxidative stress. After treatment with 1.0 mM sodium arsenite for 30 min at 37°C, Huh7 cells were subjected to immunofluorescence analysis with the indicated primary antibodies, followed by AF488-conjugated anti-goat IgG and AF594-conjugated anti-mouse or rabbit IgG. Cell nuclei were stained with DAPI (blue).

center (Szirak, Hungary), respectively. Alexa Fluor (AF)-conjugated secondary antibodies were purchased from Invitrogen (Carlsbad, CA).

Immunofluorescence microscopy. Huh7 cells were fixed in 4% paraformaldehyde in phosphate-buffered saline (PBS) for 15 min at room temperature. After cells were quenched for 10 min with PBS containing 50 mM ammonium chloride (NH_4Cl), they were permeabilized with 0.2% Triton X-100 in PBS for 10 min and blocked with PBS containing 2% bovine serum albumin (BSA) for 30 min at room temperature. The cells were then incubated with the antibodies indicated in the figure legends. Nuclei were stained with 4′,6′-diamidino-2-phenylindole (DAPI). The samples were examined by a Fluoview FV1000 laser scanning confocal microscope (Olympus, Tokyo, Japan).

Transfection, immunoprecipitation, and immunoblotting. Plasmids were transfected into 293T or Huh7 cells by use of TransIT LT1 (Mirus, Madison, WI), and cells collected at 24 h posttransfection were subjected to immunostaining, immunoprecipitation, and/or immunoblotting as described previously (24). The immunoprecipitates were boiled in sodium dodecyl sulfate (SDS) sample buffer and subjected to SDS-polyacrylamide gel electrophoresis (SDS-PAGE). The proteins were transferred to polyvinylidene difluoride membranes (Millipore, Bedford, MA) and incubated with the appropriate antibodies. The immune complexes were visualized with SuperSignal West Femto substrate (Thermo Scientific, Rockford, IL) and detected by use of an LAS-3000 image analyzer system (Fujifilm, Tokyo, Japan).

FOS-tagged purification and mass spectrometry. pCAG-Core-FOS or empty vector was transfected into 293T cells, harvested at 24 h posttransfection, washed with cold PBS, suspended in cell lysis buffer (20 mM Tris-HCl, pH 7.4, 135 mM NaCl, 1% Triton X-100, and protease inhibitor cocktail [Complete; Roche]), and centrifuged at 14,000 × *g* for 20 min at 4°C. The supernatant was pulled down using 50 μl of STrEP-Tactin Sepharose (IBA, Gottingen, Germany) equilibrated with cell lysis buffer for 2 h at 4°C. The affinity beads were washed three times with cell lysis buffer and suspended in 2× SDS-PAGE sample buffer. The proteins were subjected to SDS-PAGE, followed by Coomassie brilliant blue (CBB) staining using CBB Stain One (Nakalai Tesque, Kyoto, Japan). The gels were divided into 10 pieces, and each fraction was trypsinized and subjected to liquid chromatography-tandem mass spectrometry (LC-MS/MS) analysis to identify coimmunoprecipitated proteins. All of the proteins in gels were identified comprehensively, and the proteins detected in cells transfected with pCAG-Core-FOS but not in those with empty vector were regarded as candidates for binding partners of JEV core.

Gene silencing. A commercially available small interfering RNA (siRNA) pool targeting Caprin-1 (siGENOME SMARTpool, human Caprin1) and control nontargeting siRNA were purchased from Dharmacon (Buckinghamshire, United Kingdom) and transfected into 293T cells using Lipofectamine RNAiMAX (Invitrogen) according to the manufacturer's protocol.

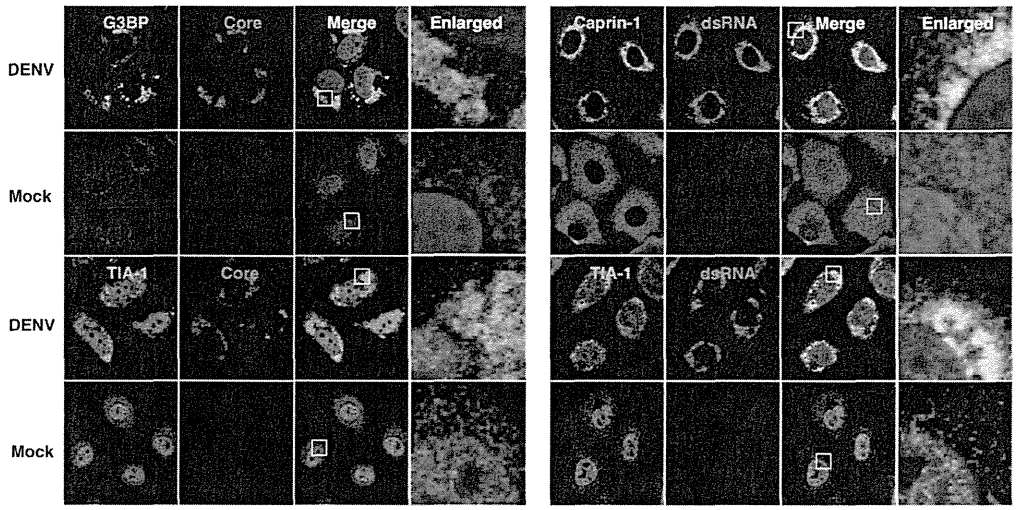

FIG 3 Subcellular localizations of the SG-associated proteins during DENV infection. Cellular localizations of G3BP, Caprin-1, and TIA-1 (green, AF488-conjugated secondary antibody) and viral components (core protein and dsRNA) (red, AF-594-conjugate secondary antibody) in Huh7 cells infected with DENV were determined by immunofluorescence analysis using the appropriate antibodies at 48 h postinfection. Cell nuclei were stained with DAPI (blue).

Preparation of recombinant proteins and GST pulldown assay. His-tagged JEV core protein (core-His) was purified as described in a previous report (25). Briefly, core-His was expressed in *Escherichia coli* (*E. coli*) Rosetta-gami 2(DE3) strain cells (Novagen-Merck) transformed with pET21b-Core-His (WT or 9798A). Bacteria grown to an optical density at 600 nm of 0.6 were induced with 0.5 mM isopropyl-β-D-thiogalactopyranoside (IPTG), incubated for 5 h at 37°C with shaking, collected by centrifugation at 6,000 × *g* for 10 min, lysed in 10 ml of bacteria lysis buffer (50 mM Tris-HCl, pH 7.4, 150 mM NaCl, 1 mM EDTA, 1% Triton X-100, and protease inhibitor cocktail [Complete; Roche]) by sonication on ice, and centrifuged at 10,000 × *g* for 15 min. The supernatant containing core-His was subjected to ammonium sulfate fractionation, followed by cation exchange chromatography with a HiTrap SP column (GE Healthcare). The eluted core-His recombinant protein was dialyzed with 50 mM Tris-HCl buffer containing 150 mM NaCl at 4°C overnight. GST-fused Caprin-1 (GST-Caprin-1) was expressed in *E. coli* BL21(DE3) cells transformed with pGEX-GST-Caprin-1. Bacteria grown to an optical density at 600 nm of 1.0 were induced with 0.1 mM IPTG, incubated for 5 h at 25°C with shaking, collected by centrifugation at 6,000 × *g* for 10 min, lysed in 10 ml of bacteria lysis buffer by sonication on ice, and centrifuged at 10,000 × *g* for 15 min. The supernatant was mixed with 200 μl of glutathione-Sepharose 4B beads (GE Healthcare) equilibrated with bacteria lysis buffer for 1 h at room temperature, and then the beads were washed five times with lysis buffer. Twenty micrograms of GST-Caprin-1 or GST was mixed with equal volumes of the purified core-His for 2 h at 4°C with gentle agitation. The beads were washed five times with bacteria lysis buffer and then suspended in SDS-PAGE sample buffer.

Mouse experiments. Experimental infections were approved by the Committee for Animal Experiment of RIMD, Osaka University (H19-2-0). Female ICR mice (3 weeks old) were purchased from CLEA Japan (Tokyo, Japan) and kept in specific pathogen-free environments. Groups of mice ($n = 10$) were intraperitoneally inoculated with 5×10^4 FFU (100 μl) of the viruses. The mice were observed for 3 weeks after inoculation to determine survival rates. To examine viral growth in the brain, 5×10^4 FFU of the viruses were intraperitoneally administered to the groups of mice ($n = 3$). At 7 days postinfection, mice were euthanized, and the cerebrums were collected. The infectious titers in the homogenates of the cerebrums were determined in Vero cells as described above.

RESULTS

JEV infection confers resistance to SG induction. To examine the formation of SGs in cells infected with JEV, Huh7 cells were infected with JEV at a multiplicity of infection (MOI) of 0.5, and the expression of JEV proteins and an accepted marker for SGs, G3BP, was determined by immunofluorescence analysis at 24 h postinfection. G3BP was mainly accumulated in the perinuclear region and partially colocalized with the JEV core protein, while only partial colocalization with the NS2B protein was also observed (Fig. 1A, left). In addition, a few small G3BP-positive foci were scattered in the cytoplasm. This accumulation of G3BP was observed in not only Huh7 cells but also other cell lines, i.e., 293T and HeLa cells, infected with JEV (Fig. 1B). However, the expression level of G3BP in cells infected with JEV was comparable to that in mock-infected cells (Fig. 1C). To further investigate SG induction by JEV infection, expression of TIA-1, another SG marker, was examined. Although accumulation of TIA-1 in the perinuclear region was not observed, a few TIA-1-positive foci were observed in the JEV-infected cells and were colocalized with G3BP and JEV NS2B, indicating that SG foci were induced in cells infected with JEV (Fig. 1D). The accumulation of G3BP and the aggregation of TIA-1, indicating SG formation, appeared at 24 h postinfection in accord with the expression of viral proteins (Fig. 1E). We further examined the dynamics of other SG-associated factors in cells infected with JEV. Each factor formed clear SGs in cells treated with sodium arsenite, a potent SG inducer eliciting oxidative stress (Fig. 2). As shown in Fig. 1F, three distinct patterns of the subcellular localization of SG components were observed. USP10 and Caprin-1 were accumulated in the perinuclear region and also formed a few small foci scattered throughout the cytoplasm, as seen for G3BP; TIA-1 and hnRNP Q formed cytoplasmic foci but were not accumulated in the perinuclear region; and subcellular localization of eIF3A and eIF4B was not changed. The cytoplasmic foci were confirmed as SGs by immunofluorescence analyses using specific antibodies to SG-associated factors (data not shown). Taken together, these results indicate that JEV infection induces accumulation of several RBPs and formation of a few SGs.

It has been shown previously that infection with WNV or DENV confers resistance to SG formation induced by sodium arsenite (15). To determine the effect of JEV infection on the SG

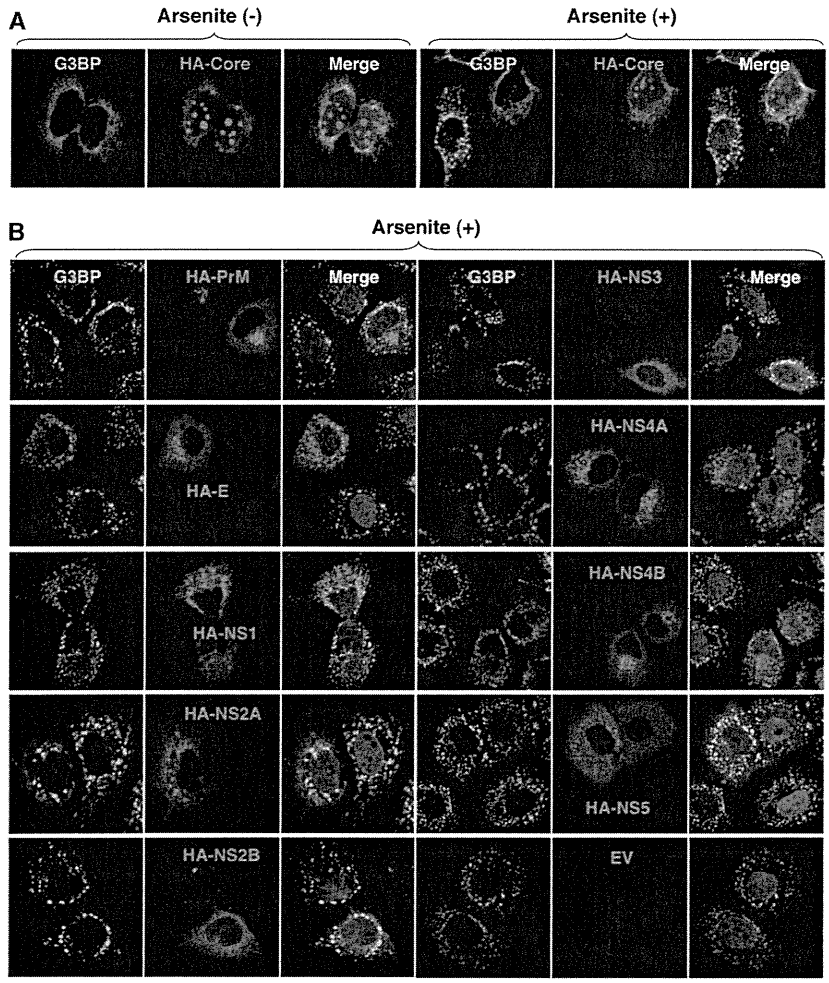

FIG 4 Inhibition of the arsenite-induced SG formation by the expression of JEV proteins. (A) Huh7 cells transfected with a plasmid, pCAGPM-HA-Core, were treated with or without 1.0 mM sodium arsenite for 30 min at 37°C, and the cellular localizations of G3BP and HA-Core were determined at 24 h posttransfection by immunofluorescence analysis with mouse anti-G3BP MAb and rat anti-HA MAb, followed by AF488-conjugated anti-mouse IgG and AF594-conjugated anti-rat IgG, respectively. Cell nuclei were stained with DAPI (blue). (B) Huh7 cells, which were separately transfected with a plasmid expressing an individual viral protein (pCAGPM-HA-JEV protein) as indicated in the figure, were treated with 1.0 mM sodium arsenite for 30 min at 37°C and subjected to an immunofluorescence assay using mouse anti-G3BP MAb and rat anti-HA MAb, followed by AF488-conjugated anti-mouse IgG and AF594-conjugated anti-rat IgG, respectively. Cell nuclei were stained with DAPI (blue).

formation induced by sodium arsenite, JEV-infected cells were treated with 0.5 mM sodium arsenite for 30 min at 24 h postinfection. Although many G3BP-positive foci were observed in mock-infected cells by the treatment with sodium arsenite, accumulation of G3BP in the perinuclear region was observed in the JEV-infected cells (Fig. 1A, right), and the numbers of G3BP-positive foci in the JEV-infected cells were less than those in the mock-infected cells (Fig. 1G). Although it has been reported that a significant reduction of the phosphorylation at Ser^{51} of eIF2α in cells treated with arsenite was induced by infection with WNV (15), the phosphorylation of eIF2α was slightly suppressed in the JEV-infected cells (Fig. 1C). Furthermore, while previous studies reported that Caprin-1 and TIA-1 were colocalized with dsRNA in cells infected with DENV (15, 26), no colocalization of G3BP or TIA-1 with the DENV core protein was observed in the present study (Fig. 3), suggesting that the mechanisms of the viral circumvention of SG formation in cells infected with JEV are different from those in cells infected with WNV and DENV.

JEV core protein suppresses SG formation induced by sodium arsenite. To elucidate the molecular mechanisms of suppression of SG formation induced by sodium arsenite during JEV infection, we tried to identify which viral protein(s) is responsible for the SG inhibition. Since G3BP was colocalized with JEV core protein, we first examined the involvement of the core protein in the perinuclear accumulation of G3BP and in the suppression of SG formation. The expression of JEV core protein alone induced the accumulation of G3BP in the perinuclear region (Fig. 4A, left panel) and suppressed sodium arsenite-induced SG formation (Fig. 4A, upper right cell in the right panel), similarly to JEV infection. In contrast, inhibition of SG formation induced by sodium arsenite was not observed in cells expressing other JEV proteins (Fig. 4B). These results suggest that JEV core protein is responsible for the circumvention of the SG formation observed in cells infected with JEV.

JEV core protein directly interacts with Caprin-1, an SG-associated cellular factor. Since JEV core protein was suggested to

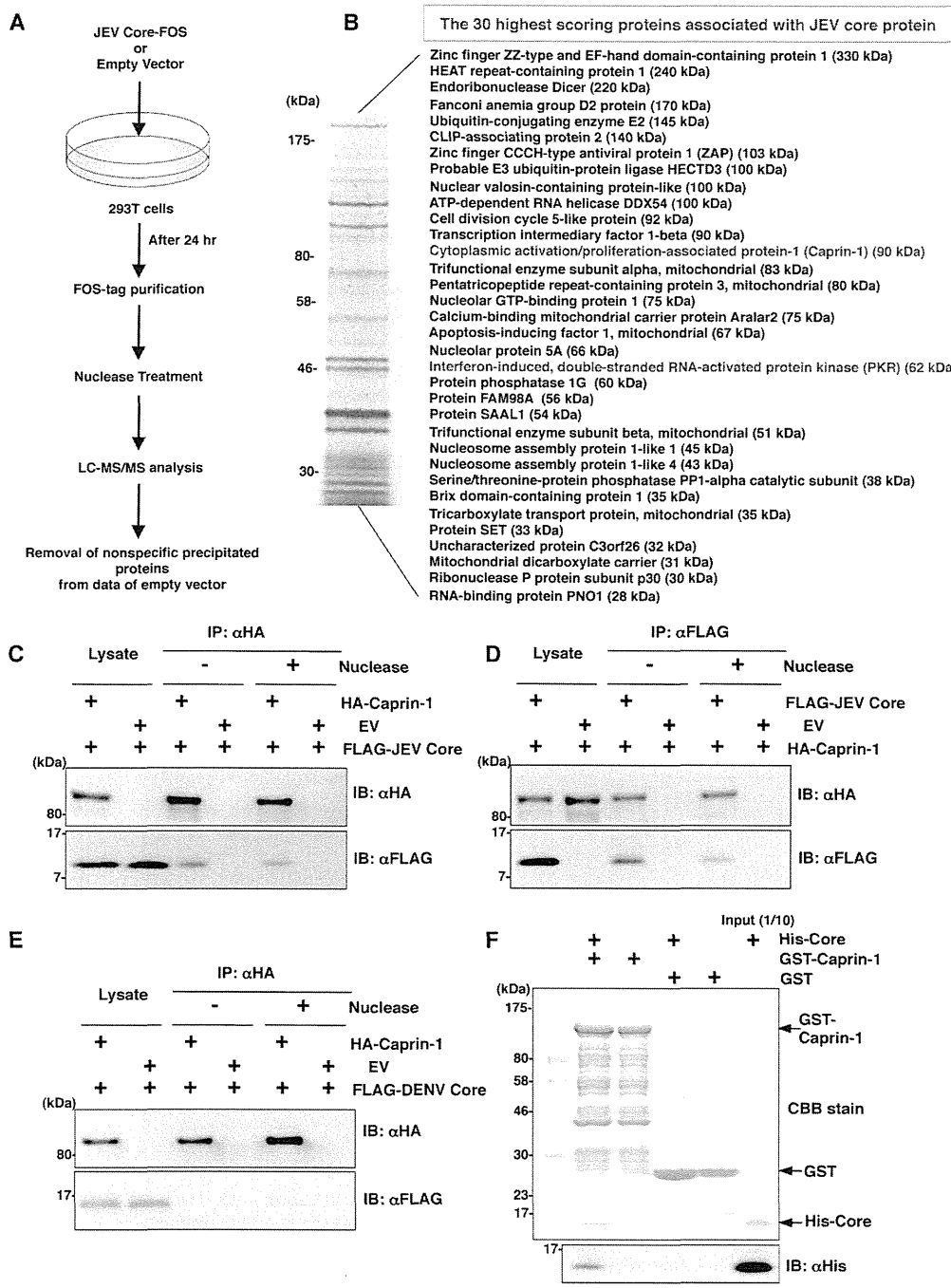

FIG 5 JEV core protein directly interacts with Caprin-1, an SG-associated cellular factor. (A) Identification of host cellular proteins associated with JEV core protein by FOS-tagged purification and LC-MS/MS analysis. Overview of the FOS-tagged purification of cellular proteins associated with JEV core protein. (B) The 30 candidate proteins as binding partners of JEV core protein exhibiting high scores are listed. PKR and Caprin-1 are indicated in red. (C and D) FLAG-JEV core protein and HA-Caprin-1 were coexpressed in 293T cells, and the cell lysates harvested at 24 h posttransfection were treated with or without micrococcal nuclease for 30 min at 37°C and immunoprecipitated (IP) with anti-HA (αHA) or anti-FLAG (αFLAG) antibody, as indicated. The precipitates were subjected to immunoblotting (IB) to detect coprecipitated counterparts. (E) FLAG-DENV core protein was coexpressed with HA-Caprin-1 in 293T cells, immunoprecipitated with anti-HA antibody, and immunoblotted with anti-HA or anti-FLAG antibody. (F) His-tagged JEV core protein was incubated with either GST-fused Caprin-1 or GST for 2 h at 4°C, and the precipitates obtained by GST pulldown assay were subjected to CBB staining and immunoblotting with anti-His antibody.

participate in the inhibition of SG formation, we tried to identify cellular factors associated with the core protein by LC-MS/MS analysis, as shown in Fig. 5A. Among the 30 factors with the best scores, two SG-associated proteins, PKR (Mascot search score, 206) and Caprin-1 (Mascot search score, 153), were identified as binding partners of JEV core protein (Fig. 5B). Although PABP1, hnRNP Q, Staufen, G3BP, and eIF4G were also identified, their scores were lower than those of PKR and Caprin-1. Because the

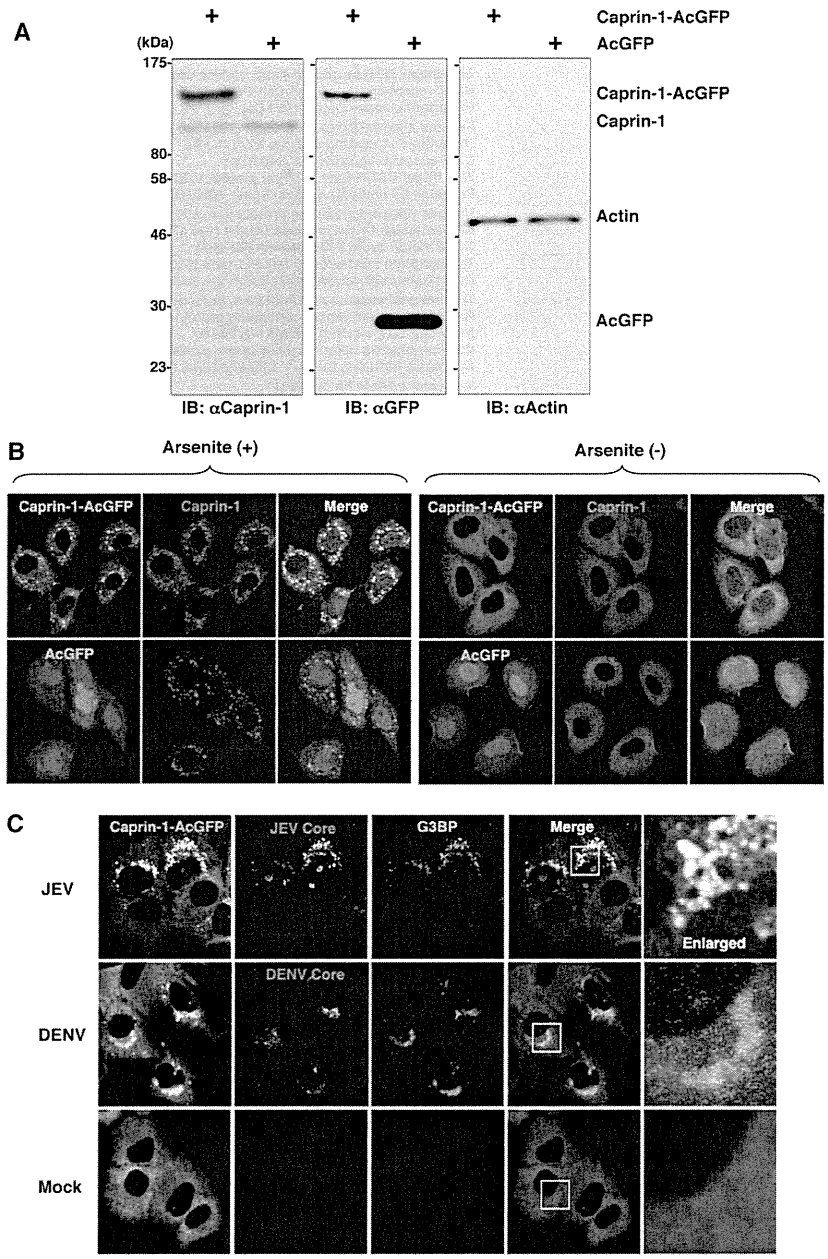

FIG 6 Caprin-1 is colocalized with the JEV core protein in the perinuclear region. (A) Expression of Caprin-1 fused with AcGFP (Caprin-1-AcGFP), Caprin-1, actin, or AcGFP in lentivirally transduced Huh7 cells was determined by immunoblotting using the appropriate antibodies. (B) Subcellular localization of Caprin-1-AcGFP or AcGFP (green) and endogenous Caprin-1 (red) in cells treated with/without 1.0 mM sodium arsenite for 30 min at 37°C was determined by immunofluorescence assay with rabbit anti-Caprin-1 PAb and AF594-conjugated anti-rabbit IgG. Cell nuclei were stained with DAPI (blue). (C) Huh7/Caprin-1-AcGFP cells were infected with either JEV or DENV at an MOI of 0.5, and the cellular localizations of JEV and DENV core (red) with Caprin-1-AcGFP and G3BP (blue) were determined at 24 h and 48 h postinfection, respectively. Cells were stained with mouse anti-G3BP MAb and rabbit anti-JEV or DENV core protein PAb, followed by AF633-conjugated anti-mouse IgG and AF594-conjugated anti-rabbit IgG, respectively, and examined by immunofluorescence analysis.

results shown in Fig. 1B suggest that the inhibition of SG formation takes place downstream of eIF2α phosphorylation, we focused on Caprin-1 as a key factor involved in the inhibition of SG formation in cells infected with JEV. To confirm the specific interaction of JEV core protein with Caprin-1, FLAG-JEV core protein and HA-Caprin-1 were coexpressed and immunoprecipitated with anti-HA or anti-FLAG antibody in the presence or absence of nuclease. FLAG-JEV core protein was coprecipitated with HA-Caprin-1 irrespective of nuclease treatment (Fig. 5C and D), suggesting that the interaction between JEV core protein and Caprin-1 is a protein-protein interaction. On the other hand, FLAG-DENV core protein was not coprecipitated with HA-Caprin-1 (Fig. 5E), indicating that the interaction with Caprin-1 was specific for JEV core protein. Next, the direct interaction be-